ELSEVIER

Available online at www.sciencedirect.com

SCIENCE DIRECT®

Applied Surface Science 224 (2004) 361–364

applied surface science

www.elsevier.com/locate/apsusc

Rigorous modeling approach to numerical simulation of SiGe HBTs

V. Palankovski[a,*], G. Röhrer[b], T. Grasser[a], S. Smirnov[a], H. Kosina[a], S. Selberherr[a]

[a]Institute for Microelectronics, TU Vienna, Gusshausstrasse 27-29, A-1040 Vienna, Austria

[b]Austriamicrosystems AG, Schloss Premstätten, A-8141 Unterpremstätten, Austria

Abstract

We present results of fully two-dimensional numerical simulations of silicon–germanium (SiGe) heterojunction bipolar transistors (HBTs) in comparison with experimental data. Among the critical modeling issues discussed in the paper, special attention is focused on the description of the anisotropic majority/minority electron mobility in strained SiGe grown in Si.
© 2003 Elsevier B.V. All rights reserved.

PACS: 85.30.Pq; 85.30.De

Keywords: SiGe; HBT; Numerical simulation; Modeling; Bandgap; Mobility

1. Introduction

Our SiGe HBT-CMOS integrated process is based on a 0.35 μm mixed-signal CMOS process and includes an additional high-performance analog-oriented HBT module. The applications reach from circuits for mobile communication to high-speed networks. Using simulation in a predictive manner has been recognized as an integral part of any advanced technology development. In order to satisfy predictive capabilities the simulation tools must capture the process as well as the device physics.

2. Physical modeling

The two-dimensional device simulator MINIMOS-NT [1] can deal with various semiconductor materials and complex geometrical structures. Previous experience gained in the area of III–V HBT modeling and simulation which lead to successful results [2] was a prerequisite to use MINIMOS-NT also for simulation of SiGe HBTs.

2.1. Bandgap and bandgap narrowing

Modeling of strained SiGe is not a trivial task, since special attention has to be focused on the stress-dependent change of the bandgap due to Ge content [3]. This effect must be separated from the dopant-dependent bandgap narrowing which for itself depends on the semiconductor material composition, the doping concentration, and the lattice temperature [4].

2.2. Carrier mobility

As the minority carrier mobility is of considerable importance for bipolar transistors, an analytical low-field mobility model which distinguishes between

* Corresponding author. Tel.: +43-1-58801-36017; fax: +43-1-58801-36099.
E-mail address: palankovski@iue.tuwien.ac.at (V. Palankovski).

0169-4332/$ – see front matter © 2003 Elsevier B.V. All rights reserved.
doi:10.1016/j.apsusc.2003.09.034

majority and minority electron mobilities has been developed [3] using Monte Carlo simulation data for electrons in Si. A similar expression is currently implemented in MINIMOS-NT:

$$\mu_n^{maj} = \frac{\mu_n^L - \mu_{mid}^{maj}}{1+(N_D/C_{mid})^{\alpha}} + \frac{\mu_{mid}^{maj} - \mu_{hi}^{maj}}{1+(N_D/C_{hi}^{maj})^{\beta}} + \mu_{hi}^{maj} \qquad (1)$$

$$\mu_n^{min} = \frac{\mu_n^L - \mu_{mid}^{min}}{1+(N_A/C_{mid})^{\alpha}} + \frac{\mu_{mid}^{min} - \mu_{hi}^{min}}{1+(N_A/C_{hi}^{min})^{\beta}} + \mu_{hi}^{min} \qquad (2)$$

$$\mu_n^{LI} = \left(\frac{1}{\mu_n^{maj}} + \frac{1}{\mu_n^{min}} - \frac{1}{\mu_n^L}\right)^{-1} \qquad (3)$$

where μ^L is the mobility for undoped material, μ_{hi} the mobility at the highest doping concentration. $\mu_{mid}^{maj}, \mu_{hi}^{maj}, \mu_{mid}^{min}, \mu_{hi}^{min}, C_{mid}, C_{hi}^{maj}, C_{hi}^{min}, \alpha$, and β are used as fitting parameters. The final low-field electron mobility μ^{LI}, which accounts for a combination of both acceptor and donor doping is given by (3). Fig. 1 demonstrates a good match between the analytical model, our Monte Carlo simulation data, and measurements [5–8] at 300 K for Si.

Monte Carlo simulation which accounts for alloy scattering and the splitting of the anisotropic conduction band valleys due to strain [9] in combination with an accurate ionized impurity scattering model [10], allowed us to obtain results for SiGe for the complete range of donor and acceptor concentrations and Ge contents x. We use the same functional form to fit the doping dependence of the in-plane mobility component for $x = 0$ and $x = 1$ (Si and strained Ge on Si). The material composition dependence is modeled by

$$\frac{1}{\mu(x)} = \frac{1-x}{\mu^{Si}} + \frac{x}{\mu^{Ge}} + \frac{(1-x)x}{C_{\mu}} \qquad (4)$$

C_{μ} is a bowing parameter which is equal to 140 and 110 cm^2/V s for doping levels below and above C_{mid}, respectively. Fig. 2 shows the in-plane minority electron mobility in $Si_{1-x}Ge_x$ as a function of x at 300 K for different acceptor doping concentrations. The model parameters used for SiGe at 300 K are summarized in Table 1.

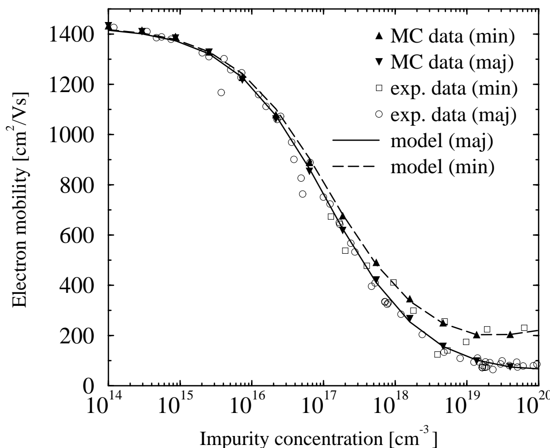

Fig. 1. Majority and minority mobility in Si at 300 K: comparison between Monte Carlo simulation data and experimental data.

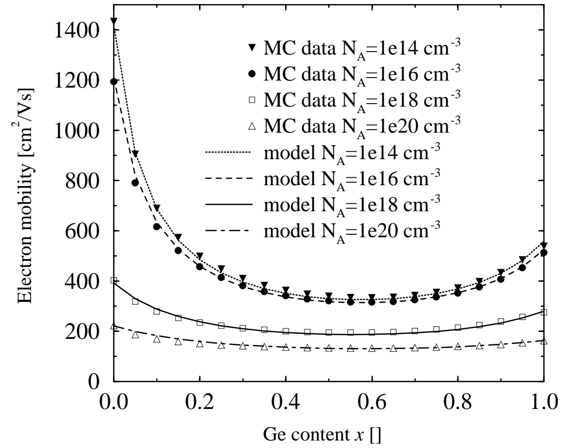

Fig. 2. Minority electron mobility in $Si_{1-x}Ge_x$ as a function of x for in-plane direction: the model gives good agreement with Monte Carlo simulation data.

Table 1
Parameter values for the majority/minority electron mobility at 300 K

Parameter	Si	Ge (on Si)	Unit
μ_n^L	1430	560	cm^2/V s
μ_{mid}^{maj}	44	80	cm^2/V s
μ_{hi}^{maj}	58	59	cm^2/V s
μ_{mid}^{min}	141	124	cm^2/V s
μ_{hi}^{min}	218	158	cm^2/V s
α	0.65	0.65	
β	2.0	2.0	
C_{mid}	1.12e17	4.0e17	cm^{-3}
C_{hi}^{maj}	1.18e20	4.9e18	cm^{-3}
C_{hi}^{min}	4.35e19	5.4e19	cm^{-3}

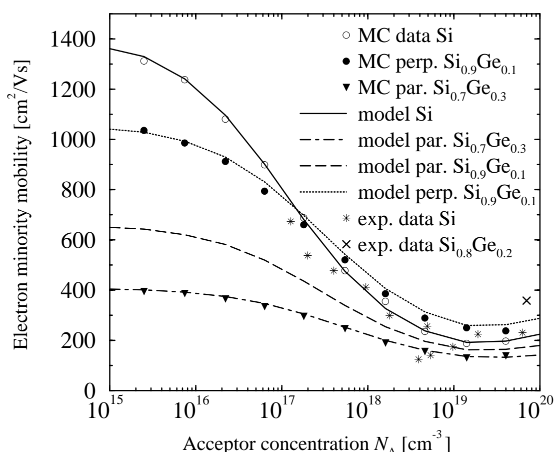

Fig. 3. Minority electron mobility in $Si_{1-x}Ge_x$ as a function of N_A and x: the model gives good agreement with measurements and Monte Carlo simulation data both for in-plane and perpendicular to the surface directions.

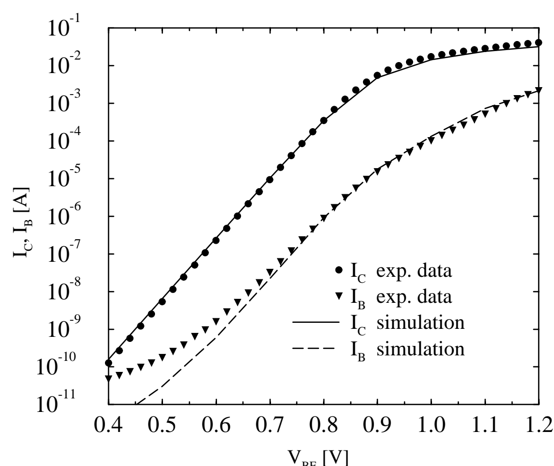

Fig. 4. Forward Gummel plots at $V_{CB} = 0$ V: comparison between measurement data and simulation at room temperature. The bandgap is one of the crucial modeling parameters.

The component of the mobility perpendicular to the surface is then obtained by a multiplication factor given by the ratio of the two mobility components. The good agreement of the model with the measured and the Monte Carlo simulation data, both for in-plane and perpendicular to the surface directions, is illustrated in Fig. 3.

3. Simulated device structure

The double-base SiGe HBT structures are CVD-grown with emitter areas of 12 μm × 0.4 μm. The base–emitter junction is formed by rapid thermal processing which causes out-diffusion of arsenic from the poly-silicon emitter layer into the crystalline silicon. The process simulation with DIOS [11] reflects real device fabrication as accurately as possible. The implant profiles as well as the annealing steps are calibrated to one-dimensional SIMS profiles. To save computational resources the simulation domain covers only one half of the real device which is symmetric and the collector-sinker and the base poly-silicon contact layer are not included in the structure.

All important physical effects, such as surface recombination, impact ionization generation, and self-heating, are properly modeled and accounted for in the simulation in order to get good agreement with measured forward (Fig. 4) and output characteristics (Fig. 5) using a concise set of models and parameters. In contrast, simulation without including self-heating effects cannot reproduce the experimental data, especially at high power levels.

The only fitting parameters used in the simulation are the contribution of doping-dependent bandgap narrowing to the conduction band (here about 80 and 20% for donor and acceptor doping, respectively), the concentration of traps in the Shockley–Read–Hall recombination model (here 10^{14} cm^{-3}), the velocity

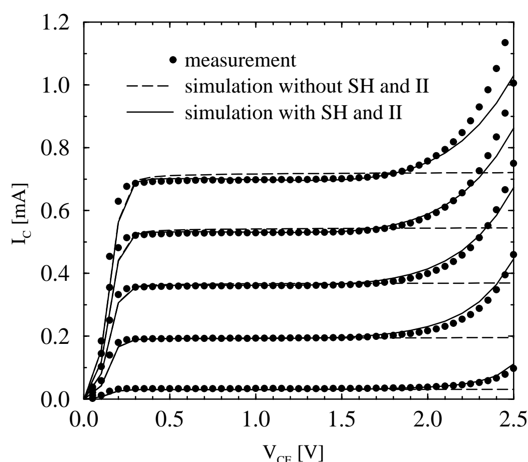

Fig. 5. Output characteristics: simulation with and without self-heating (SH) and impact ionization (II) compared to measurement data. I_B is stepped by 0.4 μA from 0.1 to 1.7 μA.

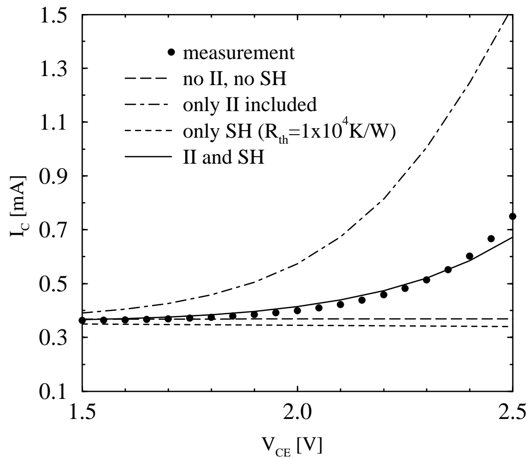

Fig. 6. Output characteristics for $I_B = 0.9$ μA: a closer look at the increasing I_C at high V_{CE} reveals the interplay between SH effect and II generation.

recombination for holes (here 8200 cm/s) in the polysilicon contact model [12] used at the emitter contact, and the substrate thermal resistance.

A closer look at the increasing collector current I_C at high collector-to-emitter voltages V_{CE} and constant base current I_B stepped by 0.4 μA from 0.1 to 1.7 μA reveals the interplay between self-heating and impact ionization (see Fig. 6). While impact ionization leads to a strong increase of I_C, self-heating decreases it. In fact, both I_C and I_B increase due to self-heating at a given bias condition. As the change is relatively higher for I_B, in order to maintain it at the same level, V_{BE} and, therefore, I_C decrease.

4. Conclusion

Critical issues for numerical modeling of SiGe devices have been discussed including accurate models for bandgap narrowing and minority/majority electron mobility in strained SiGe. Good agreement was obtained between simulation and experimental DC results (forward and output characteristics) of SiGe HBTs. The newly established models are beneficial for future process development.

Acknowledgements

The authors acknowledge the support from the Austrian Science Fund (FWF), Project P14483-MAT, and the "Christian Doppler Forschungsgesellschaft", Vienna, Austria.

References

[1] MINIMOS-NT 2.0 User's Guide, IμE, Institut für Mikroelektronik, Technische Universität Wien, Austria. http://www.iue.tuwien.ac.at/software/minimos-nt..
[2] V. Palankovski, R. Schultheis, S. Selberherr, Simulation of power heterojunction bipolar transistors on gallium arsenide, IEEE Trans. Electron Dev. 48 (6) (2001) 264–1269.
[3] J. Eberhardt, E. Kasper, Bandgap narrowing in strained SiGe on the basis of electrical measurements on Si/SiGe/Si hetero bipolar transistors, Mater. Sci. Eng. B89 (1–3) (2002) 93–96.
[4] V. Palankovski, G. Kaiblinger-Grujin, S. Selberherr, Implications of dopant-dependent low-field mobility and band gap narrowing on the bipolar device performance, J. Phys. IV 8 (3) (1998) 91–94.
[5] G. Masetti, M. Severi, S. Solmi, Modeling of carrier mobility against carrier concentration in arsenic-, phosphorus- and boron-doped silicon, IEEE Trans. Electron Dev. ED-30 (7) (1983) 764–769.
[6] K. Wolfstirn, Hole and electron mobilities in doped silicon from radiochemical and conductivity measurements, J. Phys. Chem. Solids 16 (3–4) (1960) 279–284.
[7] S.E. Swirhun, D.E. Kane, R.M. Swanson, Measurements of electron lifetime, electron mobility and band-gap narrowing in heavily doped p-type silicon, in: Tech. Digest IEDM, San Francicso (1986), pp. 24–27.
[8] I.Y. Leu, A. Neugroschel, Minority-carrier transport parameters in heavily doped p-type silicon at 296 and 77 K, IEEE Trans. Electron Dev. 40 (10) (1993) 1872–1875.
[9] S. Smirnov, H. Kosina, S. Selberherr, Investigation of the electron mobility in strained $Si_{1-x}Ge_x$ at high Ge composition, in: Proceedings of the International Conference on Simulation of Semiconductor Processes and Devices, Kyoto, 2002, pp. 29–32.
[10] H. Kosina, G. Kaiblinger-Grujin, Ionized-impurity scattering of majority electrons in silicon, Solid State Electron. 42 (3) (1998) 31–338.
[11] ISE, Integrated Systems Engineering AG, Zürich, DIOS-ISE, ISE TCAD Release 8.0, 2002.
[12] Z. Yu, B. Ricco, R. Dutton, A comprehensive analytical and numerical model of polysilicon emitter contacts in bipolar transistors, IEEE Trans. Electron Dev. 31 (6) (1984) 773–784.